Contents lists available at ScienceDirect

Heliyon

Foam glasses made from green bottle glass and sugar beet factory lime as a foaming agent

Veljko Savić [a,*], Vladimir Topalović [a], Jelena Nikolić [a], Sanja Jevtić [b],
Nebojša Manić [c], Mirko Komatina [c], Srđan Matijašević [a], Snežana Grujić [b]

[a] *Institute for Technology of Nuclear and Other Mineral Raw Materials, Bulevar Franš D'Eperea 86, 11000, Belgrade, Serbia*
[b] *University of Belgrade, Faculty of Technology and Metallurgy, Karnegijeva 4, 11000, Belgrade, Serbia*
[c] *University of Belgrade, Faculty of Mechanical Engineering, Kraljice Marije 16, 11000, Belgrade, Serbia*

ABSTRACT

Great waste production alongside limited natural resources represents huge environmental and economic problems worldwide. Sustainable waste management and industrial production can reduce pollution and gain some economic benefits. Eco-friendly thermal insulators such as foam glasses can be produced using secondary raw materials in open-loop recycling. Foam glasses were successfully produced using green bottle glass and sugar beet factory lime (SBFL), $CaCO_3$-rich waste as a novel foaming agent. Glass powder was mixed with different amounts of SBFL, uniaxially pressed at 20 MPa, and sintered at different temperatures. The influence of sintering temperature and the addition of a foaming agent was examined. Obtained samples were mechanically, thermally, and microstructurally characterized. Results showed that samples sintered at 800 °C have the best properties. Obtained foam glasses can be used in a variety of industries where thermal insulation, non-flammability, and non-toxic materials are required.

1. Introduction

The glass industry was among the first to start collecting and recycling its packaging and achieved one of the highest recycling rates. Glass from containers, such as bottles and jars, can be recycled almost completely and indefinitely, without any loss in its quality or purity. Recycling waste glass for the production of new glassy products leads to a lower amount of waste glass disposed of in landfills, reduces the utilization of natural materials, and promotes the reduction of pollution [1]. In the European Union, the average glass recycling rate was 74% in 2018. This means that over 11.6 million tons of glass bottles are collected, and recycled into food-grade quality material for the production of new glass containers [2]. In the United States, the situation is far worse. In 2018., only 25% of glass waste was recycled [3]. In 2021. only 46% of glass packing waste was recycled in Serbia. The Serbian Environmental Protection Agency has set a target for recycling rates in 2024. at 48% [4]. Waste glass packing can be recycled through closed-loop and open-loop recycling [5]. Closed-loop recycling means that waste glass is returned to glass manufacturers to be re-melted into products similar to the original. Sometimes, the impact of the transportation distance on the environment can be more devastating than the benefits of glass incorporation in closed-loop recycling [6]. When waste glasses show a higher level of contamination, making them unusable for closed-loop recycling, some environmental benefits can still be achieved through open-loop recycling [5]. Waste glass, as

---

a secondary raw material in open-loop recycling, can be utilized as aggregate for asphalt [7], for the production of high-performance concrete [8], for radiation shielding [9], for glass-ceramic preparation [10], etc. One of the promising research fields for the utilization of waste glass is the production of foam glasses for thermal insulation.

Thermal insulation materials are mostly used in the building industry. Buildings' envelopes are considered a main element for improving their thermal performance because they account for 50–60% of all heat transfer [11,12]. Using thermal insulators lessens the need for heating, ventilation, and air conditioning systems. As a result, it saves energy and uses fewer natural resources. Profits, environmentally friendly materials, extending indoor thermal comfort times, lowering noise levels, fire prevention, and others are benefits of thermal insulation applications [13].

Foam glasses are porous materials consisting of a solid glass matrix and gas phase, in the pores [14]. As a thermal insulator, foam glass is competing with polymeric materials. Foam glasses have some superior properties compared to polymer foams: it has greater mechanical strength, lower flammability, and high chemical durability. The most common way for foam glass production is sintering with simultaneous gas release, where glass powder is mixed with a foaming agent and then the mixture is pressed to obtain pellets. Pellets are heated above the glass-softening temperature, where sintering of the glass powder and release of gases from the foaming agent occurs [15]. Released gas expands raw pellets and forms a porous structure. There are two ways of gas forming, by redox reaction, and by thermal decomposition. Foaming by redox reaction usually happens by carbon black or SiC oxidation with oxygen present in the entrapped, inter-particle atmosphere and with the addition of oxidizing agents. Oxidizing agents, such as Fe_2O_3 [16], MnO_2, Mn_2O_3, and Mn_3O_4 [17], and Co_3O_4 [18], are transition metals in higher oxidation states that may be reduced to lower oxidation states to promote the appropriate amount of oxygen during the foaming process. Sodium and calcium carbonate are mostly used in the process of foaming by thermal decomposition [19,20]. During the sintering process, the glass softens, and the carbonate particles decompose to sodium/calcium oxide with the simultaneous release of gaseous carbon dioxide. The sodium/calcium oxide is incorporated into the softened glass mass and acts as a glass modifier, changing the glass's viscosity. The CO_2 gas which is released can escape or be trapped in the viscous glass mass depending on the extent of sintering. In the well-sintered body, the CO_2 gas will be trapped and its pressure will gradually increase, forcing the softened glass mass to expand [14].

There are numerous studies on foam glasses, but only a few where both the glass matrix and the foaming agents, used for production, are secondary raw materials. Souza et al. used discarded glass bottles and eggshells as raw materials. Mixtures were sintered at 900 °C for 30 min and obtained foam glasses had porosities between 60 and 95% with thermal conductivities between 0.177 and 0.055 W/(m·K) [21]. The synthesis of foam glass from amber glass and pork bone was investigated by Gong et al. [22]. The powder mixture was sintered at 850 °C for 10 min and foam glasses with high flexural strength (between 16.71 ± 1.73 and 29.69 ± 3.23 MPa) were synthesized. Assefi et al. [23] researched the production of foam glass from LCD panels of TVs as the glass matrix and manganese dioxide from scrap alkaline batteries and chemical grade sodium carbonate as foaming agents, respectively. Obtained foam glasses had a compressive strength ranging from 28.7 to 8.7 MPa and an apparent density of 1.86–0.76 g/cm^3 and a thermal conductivity of 0.22 W/(m·K) at the density of 0.85 g/cm^3. Arcaro et al. [24] made foam glasses from transparent glass bottles and banana leaves. The obtained foam glasses have porosities between 58.5 and 87.5%, compressive strength ranging between 1.17 and 3.50 MPa, and thermal conductivity ranging between 0.06 and 0.15 W/(m·K). Stochero et al. [25] produced foam glasses from discarded glass bottles and pine scales as foaming agent. The samples had porosities between 78 and 86% with thermal conductivities between 0.072 and 0.093 W/(m·K) and compressive mechanical strength between 0.2 and 3.4 MPa. Souza et al. [26] investigated the production of foam glasses made from discarded glass bottles and ornamental stone processing waste as pore-forming agents. Produced foams are with properties compared to commercial ones, porosities are between 75% and 90%, thermal conductivities between 0.04 and 0.07 W/(m·K), and compressive strength between 1.0 and 4.3 MPa.

Sugar production from sugar beets passes through several steps. Sugar beet is sliced and sent to a diffuser in which the juice is extracted from the beet cells. In this process raw juice (that contains around 14–15% dry substance) is obtained. The raw juice is then sent to the next stage, i.e., the purification stage [27]. In this stage, the lime milk ($Ca(OH)_2$), is used to treat heated raw juice to destabilize and precipitate the suspended and colloidal particles of non-sugars. After that, the mixture is treated with CO_2 gas to adjust the juice pH and precipitate the lime (as $CaCO_3$) with impurities [28,29]. Following purification, thin juice proceeds to the next stage of sugar manufacture.

$CaCO_3$ is obtained as a byproduct of sugar production. It is called defection lime or sugar beet factory lime (SBFL) [29]. SBFL doesn't have wide utilization. It is mostly used as a pH adjuster or soil fertilizer [27], as epoxy composites [30], or as a filler for plastic, rubber, or paper [31]. Most factories still discharge it in lime ponds or open dumping places which isn't an environmentally friendly methodology [27].

SBFL is $CaCO_3$-rich waste that can be used as a foaming agent in foam glass production. The green bottle glass as a glass matrix and SBFL as a foaming agent are used in this research to synthesize foam glasses. The influence addition of the foaming agent on microstructure, mechanical strength, and thermal conductivity was investigated at different sintering temperatures.

2. Materials and methods

2.1. Preparation and characterization of raw materials

Discarded green beer bottles were used as a glass raw material. The beer bottles were first crushed in agate mortar into a cullet and then pulverized into fine particles with TENCAN planetary mill at 400 rpm for 60 min. Obtained glass powder was sieved to obtain glass powder particles size under 48 μm.

Sugar beet factory lime (SBFL), used as a foaming agent, was obtained from a sugar factory in Crvenka, Serbia. SBFL was dried in an

oven at 110 °C to remove moisture, then crushed in an agate mortar and sieved to particles size under 48 μm.

The chemical compositions of glass and SBFL were determined using gravimetric and spectroscopic methods (AAS Analyst 300). Content of SiO_2 and l. o.i. (loss on ignition at 900 °C) were determined gravimetrically, while the content of oxides Al_2O_3, CaO, MgO, Na_2O, Fe_2O_3, MnO, and Cr_2O_3, was determined by analyzing the content of their cations in solution by the method of atomic absorption spectrometry (AAS).

A hot-stage microscope (HSM) with a Canon camera was used to determine the behavior of the glass powder during sintering. The cylinder obtained by pressing the glass powder (<48 μm) was heated at the heating rate of 10 °C/min. The photos of the characteristic shapes were taken during heating and were used to calculate the sample area at different temperatures. A ratio of A/A_0 was used as a shrinkage measure, where A_0 is the initial area of the sample and A is the area at temperature T.

Thermogravimetry (TG) and derivative thermogravimetry (DTG) analysis of the SBFL was performed using SDT Q600 v7.0 Build 84 TG A/DSC TA Instruments device. The sample was heated in a static air atmosphere in alumina sample pans at the heating rate of 10 °C/min up to $T = 900$ °C.

2.2. Preparation and characterization of foam glass

Glass powder was mixed with SBFL, a source of calcium carbonate, to prepare three mixtures containing 2.5 mass% (S2.5), 5 mass% (S5), and 7.5 mass% (S7.5) of $CaCO_3$, respectively. Mixtures were mixed in TENCAN planetary mill at 400 rpm for 30 min to obtain homogeneity. The mixture was uniaxially pressed in a Manfredi C 95 laboratory hydraulic press at 20 MPa with the addition of 5% moisture as a binder. The obtained pellets had 10 g, 30 mm in diameter, and 6 mm thickness and were placed in an electric furnace Carbolite CWF 13/13. Samples were heated at $T = 750, 800, 850,$ and 900 °C for 30 min at a heating rate of 10 °C/min. Synthesized samples were polished using SiC abrasive paper to obtain parallel surfaces of pellets.

Crystalline phases in the samples were identified using a Philips PW-1710 automated diffractometer with a Cu tube operated at 40 kV and 30 mA.

The true density (ρ_t) of glass powder was measured using the pycnometer method [32] and the geometrical density (ρ_g) of the foam glass samples was calculated from the mass-volume ratio of the samples. The porosity (ε) of the samples was estimated using equation (1):

$$\varepsilon = \left(1 - \rho_g / \rho_t\right) \times 100 \tag{1}$$

A compression test on three samples was used to determine the mechanical strength of samples using the Compressive strength measurement apparatus (100 (kN) cell load capacity, Alfred J Amsler & Co, Germany).

The thermal conductivity of samples was determined in a thermal conductivity analyzer, model TCi Thermal Conductivity Analyzer, *C*-THERM Technologies Ltda., CA (according to ASTM D7984-21 [33]). The measurement was performed at room temperature. Five measurements were performed on each of the samples.

The morphology and pore structure of the foam glasses was investigated by photographing samples and analyzing them on the ImageJ software [34]. The polished surface of the samples was examined, and more than 1000 pores were analyzed to ensure statistical significance.

3. Results and discussion

3.1. Characterization of raw materials

Table 1 Shows the results of the chemical analysis of the green bottle glass.

The chemical composition of the glass is typical for soda-lime silicate glasses used for the production of bottles. SBFL is obtained in a filter press during raw juice purification and typically contains about 30% of moisture. The main component of dried SBFL is calcium carbonate, but it also contains a low amount of nitrogen compounds, minerals, and sucrose [35]. Chemical analysis of dried SBFL shows that it consists of 69.21% $CaCO_3$.

The geometric shapes of the fixed viscosity points [36] during the heating of glass powder are given in Table 2.

The temperature of the first shrinkage (T_{FS}) is the one at which the sample shrinks to roughly 3–5% of its initial area and the usual viscosity is $10^{8.1\pm0.1}$ Pa s. The T_D is the viscosity point of $10^{5.3\pm0.1}$ Pa s, where the first signs of softening may be observed when the sample edges are rounded. At T_S the sample becomes spherical and viscosity is $10^{4.4\pm0.1}$ Pa s. The half ball temperature, T_{HB}, corresponds to a viscosity of $10^{3.1\pm0.1}$ Pa s, and the flow temperature (T_F) is the temperature of molten glass where viscosity is $10^{2.4\pm0.1}$ Pa s [36,37]. Based on the results given in Table 2, parameters for the Vogel–Fulcher–Tammann equation (*A*, *B*, and T_0(K)) were determined [36].

Glass powder densification begins at about 590 °C, while glass softening occurs around 700 °C (Fig. 2a.). Glass begins to expand

Table 1
Chemical composition of the green bottle glass.

Oxides	SiO_2	Al_2O_3	CaO	MgO	Na_2O	Fe_2O_3	MnO	Cr_2O_3	L.o.i.
mass %	71.8	2.46	10.21	2.05	12.74	0.42	0.0121	0.11	0.62

Table 2
Experimental images of the fixed viscosities points.

	Temperature, °C	Viscosity, Pa s	HSM image
Starting sample	25	/	
Temperature of the first shrinkage, T_{FS}	590	$10^{8.1}$	
Softening temperature, T_D	700	$10^{5.3}$	
Sphere temperature, T_S	800	$10^{4.4}$	
Half-ball temperature, T_{HB}	850	$10^{3.1}$	
Flow temperature, T_F	1020	$10^{2.4}$	

above 800 °C. Fig. 2b indicates weight loss at 130 °C owing to water evaporation, and at 310 and 460 °C because of the decomposition of organic components contained in the raw juice purification sample. The sample begins to decompose significantly at about 600 °C, and the largest weight loss (~37%) occurs at around 800 °C. There is no weight loss in the sample after 800 °C. This is very similar to the temperature interval for pure $CaCO_3$ decomposition [38].

In the literature can be found that foaming of soda lime silicate glasses occurs in a viscosity window between 10^7-10^3 Pa s [15]. Based on these results, 2.5 mass% (S2.5), 5 mass% (S5), and 7.5 mass% (S7.5) of $CaCO_3$ from SBFL as a foaming agent are used to investigate foaming agent addition on properties of foam glasses sintered at 750, 800, 850, and 900 °C, where the viscosity of glass is in $10^{4.5}$–$10^{3.1}$ Pa s range, determined from Fig. 1.

3.2. Characterization of foam glasses

3.2.1. XRD analysis

Sodium-calcium silicate glasses used as packaging have a low tendency towards crystallization. Glass powder has a greater tendency towards crystallization than bulk glass of the same composition. The crystallization tendency changes with surface roughness. The nucleation trend is higher on unpolished surfaces [39]. Pressed glass powder with the foaming agent has many nucleation sites so nucleation and crystallization can occur at a temperature range where the foaming agent decomposes and viscous sintering of glass powder occurs. The crystallinity rate and the type of the crystalline phases depend on the chemical composition of the mixture as well as the sintering temperature, and both have an impact on the properties of the resulting foam glass. Fig. 3 Shows XRD diffractograms of obtained foam glasses. These diffractograms reveal a broad XRD peak between 14° and 40° typical of silica-based glasses, as well as diffraction peaks indicating crystalline phases. The intensity of a broad peak between 14° and 40° decreases with increasing foaming agent content, indicating that as the foaming agent content increases, so does the crystallinity of the samples. This can be confirmed by the increased number and intensity of diffraction peaks indicating certain crystalline phases. The same trend can be observed with the rise in sintering temperature. The greater the sintering temperature, the higher the amount of crystalline phase.

Diopside is the most dominant crystalline phase formed after sintering in the temperature range 750–900 °C ($10^{4.5}$–$10^{3.1}$ Pa s). In sample S7.5 sintered at 750 °C, wollastonite was detected next to the diopside. In all samples regardless of foaming agent addition
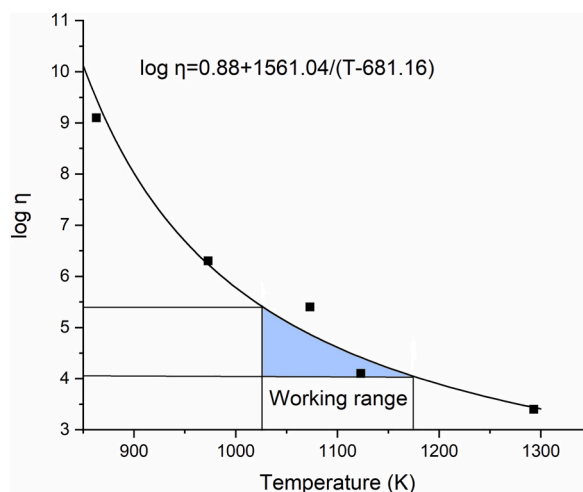

Fig. 1. Viscosity curve of glass powder obtained from fixed viscosity points determined by HSM.
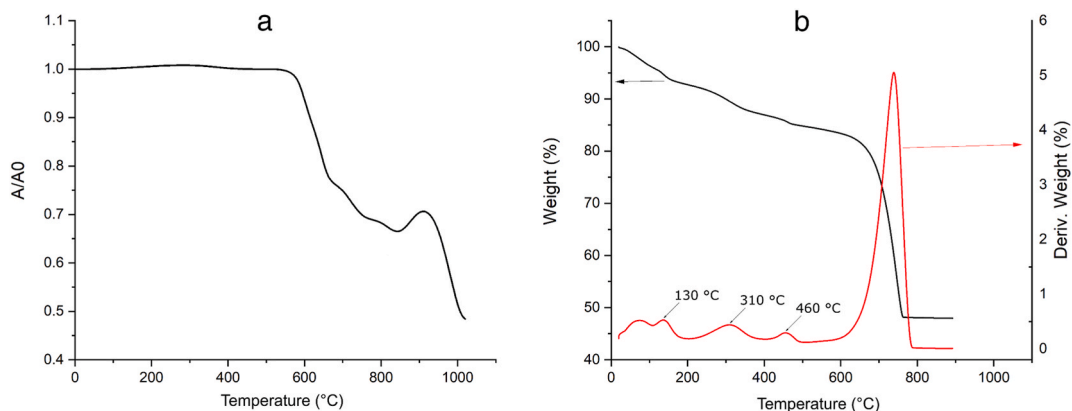
Fig. 2. A) HSM of the green bottle glass, granulation of powder <48 μm, heating rate $v = 10$ °C/min; b) TG/DTG of SBFL granulation of powder <48 μm, heating rate $\beta = 10$°C/min. (For interpretation of the references to colour in this figure legend, the reader is referred to the Web version of this article.)
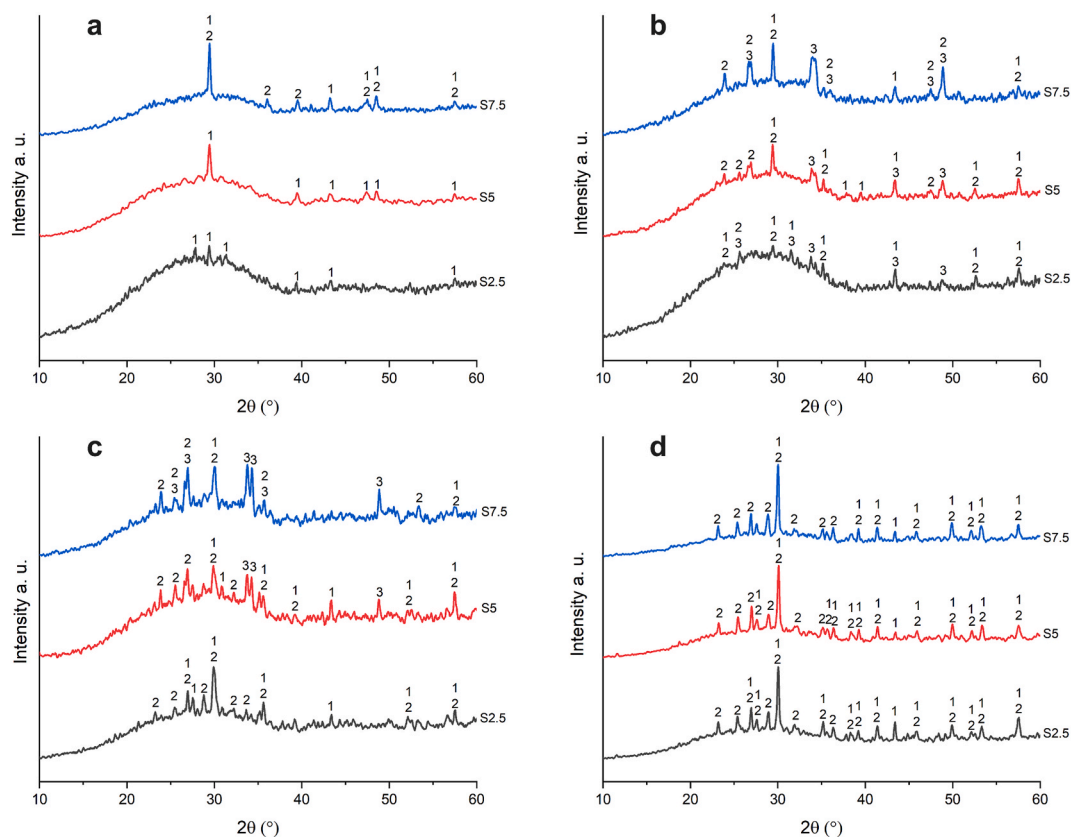

Fig. 3. XRD diffractograms of foam glasses sintered at a) 750 °C, b) 800 °C, c) 850 °C, and d) 900 °C, 1- Diopside ($CaMgSi_2O_6$) 2- Wollastonite ($CaSiO_3$), 3- Merwinite ($Ca_3Mg(SiO_4)_2$).

wollastonite crystals were identified in the temperature range 800–900 °C ($10^{3.9}$–$10^{3.1}$ Pa s). The appearance of merwinite has been confirmed after sintering at 800 °C and 850 °C while at 900 °C only diopside and wollastonite crystalline phases are detected in the samples. It is evident that in all samples, regardless of sintering temperature, non-stoichiometric crystallization occurs.

In the sample S2.5 sintered at 750 °C the crystallization is at the beginning and in Fig. 3a only peaks corresponding to diopside can be seen. Samples S5 and S7.5 sintered at the same temperature have higher levels of crystallinity. Increasing the amount of $CaCO_3$ tends to enhance crystallization. This is probably a consequence of the influence of CaO (decomposition product) on the viscosity. CaO breaks down the silica network and decreases viscosity so the crystallization will be enhanced. Also, during non-stoichiometric

crystallization, the chemical composition of the residual glass matrix continuously changes with time. These compositional shifts, resulting from the formation of two main phases (diopside and wollastonite), probably lead to a decrease in viscosity and an additional increase in crystallization.

3.2.2. Mechanical properties of foam glasses

The porosity of foam glass has a strong influence on the mechanical and thermal properties of foam glass. It is well known that as the porosity of the sample increases, its mechanical strength decreases. Table 3 Shows the total porosity and compressive strength of foam glasses.

Commercial foam glasses usually have compressive strength between 0.4 and 6 MPa according to Scheffler and Colombo [14], and foam glasses produced in this research fit into a defined range. It can be seen from Table 3., as is expected, that at all sintering temperatures, the compressive strength of foam glasses increases as porosity decreases. It is evident that increasing the addition of $CaCO_3$ leads to a decrease in porosity at all sintering temperatures, implying that samples S5 and S7.5 contain more than the optimal amount of $CaCO_3$.

At 750 °C ($10^{4.5}$ Pa s), the sintering is incomplete, and the resulting structure permits gases from carbonate decomposition to escape into the atmosphere. The sintering temperature of 750 °C is insufficient to completely decompose all SBFL, which has a maximum mass loss at 800 °C (Fig. 2b). When compared to samples sintered at higher temperatures, those sintered at 750 °C had lesser porosity. The higher compressive strength of S2.5 sintered at 750 °C compared to other sintering temperatures is a consequence of poorly developed pores in the sample [21].

Sample S2.5 had a porosity of roughly 90% at higher sintering temperatures of 800–850 °C ($10^{3.9}$-$10^{3.4}$ Pa s), indicating that the well-sintered structure prevents gases from carbonate decomposition from exiting. Sintering is difficult for samples S5 and S7.5 because they have more than the appropriate amount of $CaCO_3$, and extra gases might escape the structure, reducing porosity. Also, an increased amount of $CaCO_3$ tends to enhance crystallization, which in turn is expected to increase the overall viscosity of the system, hindering the sintering and foaming (expansion). Therefore, samples S5 and S7.5 have lower porosity than samples S2.5. Reduced porosity combined with increased crystallinity (Fig. 3) increases compressive strength [40]. At the 900 °C ($10^{3.1}$ Pa s) sintering temperature, due to low viscosity, gasses from decomposition escape easily, resulting in the collapse of the foam so the porosity of the samples S2.5 is lower than for those sintered at 800–850 °C.

Although all samples S7.5 (Table 3.) have much greater mechanical strength than samples S2.5 and S5, they have a porosity of less than 70%, which is insufficient for thermal insulation due to increased thermal conductivity [26].

3.2.3. Thermal properties of foam glasses

The dominant mechanism for heat transfer in foam glasses is conduction (Fourier's law). The density and porosity of the foam glass have the most influence on its thermal conductivity [21]. Fig. 4 Depicts the influence of density on thermal conductivity at different sintering temperatures.

The thermal conductivity of the samples changes in a manner similar to the density changes as the amount of foaming agent is increased. When the amount of foaming agent is increased, both the thermal conductivity and density of the samples increase at all sintering temperatures. In general, reduced density (and larger porosity) leads to decreased thermal conductivity at all sintering temperatures. The best thermal insulation properties have a S2.5 sintered at 800 °C (density 0.211 g/cm^3 and thermal conductivity 0.043 W/(m·K). The increased amount of $CaCO_3$ (S5) at the same sintering temperature leads to the rise of density to 0.521 g/cm^3 and an increase of thermal conductivity by 25% (0.058 W/(m·K)), while compressive strength improves by 37%, from 0.63 MPa to 0.99 MPa (Table 3). According to all previous analyses of the density, compressive strength, and thermal conductivity, of the produced foam glasses, the amount of foaming agent and sintering temperature has a significant impact on its mechanical and thermal properties. Depending on the required properties of the material for usage as an insulator, foam glasses with various combinations of properties can be produced by altering the amount of foaming agent, whether is more important to have improved compressive strength or thermal conductivity. A sintering temperature of 750 °C is not optimal for foam glasses production as discussed in section 3.2.2., and a further increase in sintering temperature (to 850 °C and 900 °C) does not improve the properties of foam glasses (thermal conductivity

Table 3
Total porosity and compressive strength of obtained foam glasses.

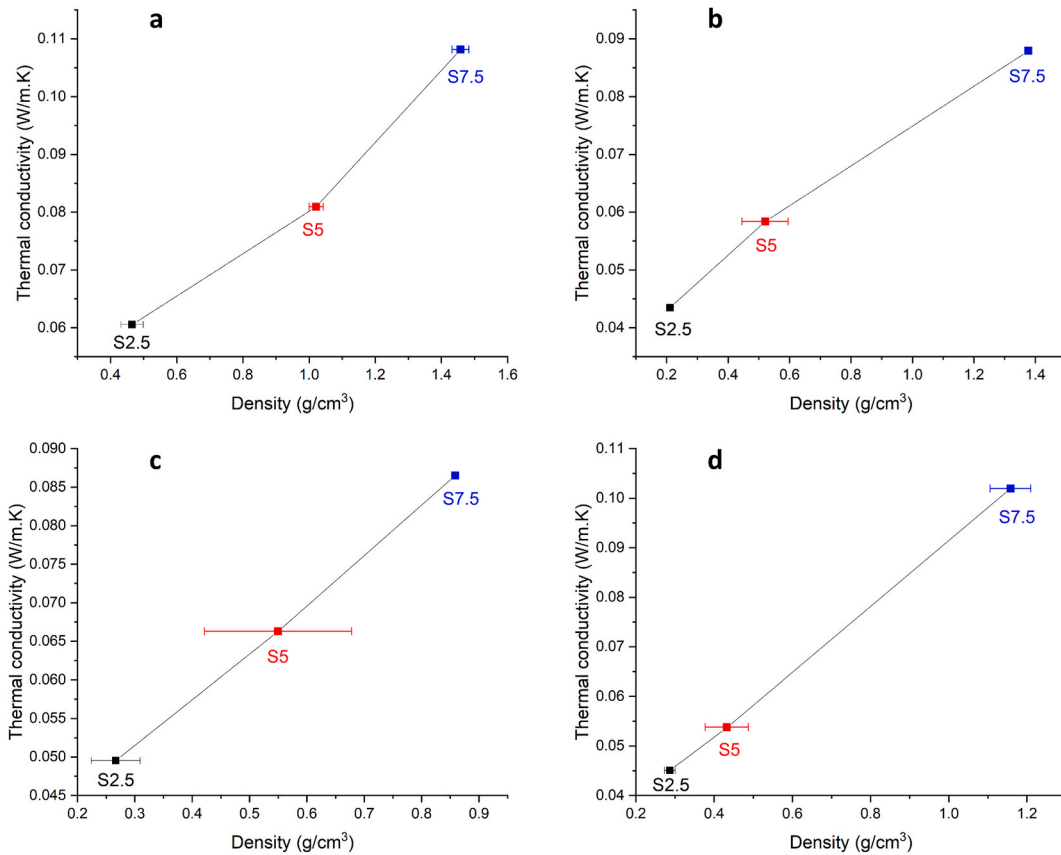| Sintering temperature, °C	Name	Porosity, %	Compressive strength, MPa
750	S2.5	82.1 ± 1.3	0.90 ± 0.16
	S5	60.6 ± 0.8	0.93 ± 0.11
	S7.5	43.8 ± 0.6	3.38 ± 0.24
800	S2.5	91.9 ± 0.1	0.63 ± 0.04
	S5	79.9 ± 2.9	0.99 ± 0.14
	S7.5	46.0 ± 0.4	2.16 ± 0.12
850	S2.5	89.7 ± 1.7	0.48 ± 0.07
	S5	78.8 ± 4.9	1.03 ± 0.05
	S7.5	66.9 ± 0.1	1.40 ± 0.24
900	S2.5	89.0 ± 0.5	0.76 ± 0.07
	S5	83.3 ± 2.1	1.37 ± 0.28
	S7.5	55.4 ± 2.0	1.93 ± 0.44

Fig. 4. Density and thermal conductivity of samples sintered at: a) 750 °C b) 800 °C, c) 850 °C and d) 900 °C.

of 0.050 and 0.045 W/(m·K) for Samples S2.5, and 0.066 and 0.054 W/(m·K) for Samples S5, respectively). Therefore, increasing the sintering temperature beyond 800 °C will not improve thermal insulation properties, and more importantly, will use more energy and raise production costs.

3.2.4. Microstructural properties of foam glasses

Apart from phase composition, density, and total porosity, pore size distribution has a considerable impact on the mechanical and thermal properties of foam glasses. Fig. 5 Presents digital images of synthesized foam glasses with their pore size distribution.

Fig. 5 Shows that the polished surface of S2.5 sintered at 750 °C exhibits a few larger pores among tiny pores. Pore size heterogeneity might result from particle agglomeration, an inhomogeneous distribution of foaming agents, or a temperature difference in the furnace [14]. The pore structure of samples S5 and S7.5 has a homogeneous size distribution, with the median pore size of samples S5 and S7.5 193.4 μm and 146 μm, respectively.

An increase in sintering temperature to 800 °C leads to better development of pores and their increase in size. Samples S2.5 and S5 had d_{90} pore diameters that are similar (about 1300 μm). S2.5, with a porosity of 91.9%, has a 32% larger median pore size than S5 (423 μm vs. 291 μm), with a porosity of 79.9%. Pore size has a significant effect on the properties of produced foams. In this case, S2.5 has a somewhat lower thermal conductivity than S5 (0.044 W/(m K) vs. 0.058 W/(m K)), but its compressive strength is just 0.62 MPa compared to 0.98 MPa for S5. S7.5 has the same undeveloped pores as S7.5 sintered at 750 °C, with a median size of 169 μm. Samples sintered at 850 °C and 900 °C follow the same pattern as samples sintered at 800 °C. Sample S2.5 sintered at 850 °C has a median pore size of 379 μm and a compressive strength of 0.48 MPa, whereas S5 has a compressive strength of 1.03 MPa and a 25% lower median pore size (286 μm). At 900 °C, the median pore size is decreased from 310 μm in S2.5–274 μm in S5. Samples S7.5 sintered at 850 and 900 °C exhibit larger pores than at lower sintering temperatures. At higher sintering temperatures internal pressure of released CO_2 increases and the viscosity of glass decreases, and the pore size tends to increase with the coalescence of smaller pores leading to greater pore size.

Generally, an increase in internal pressure leads to greater pore size and more gaseous phase in the sample which causes thinner pore walls in the foam glass sample. More gaseous phase improves thermal insulation properties, but it has a negative effect on compressive strength because the thinner the pore wall, the poorer mechanical properties. Foam glass may be tailored to desired unique properties by adjusting the amount of foaming agent and sintering temperature.
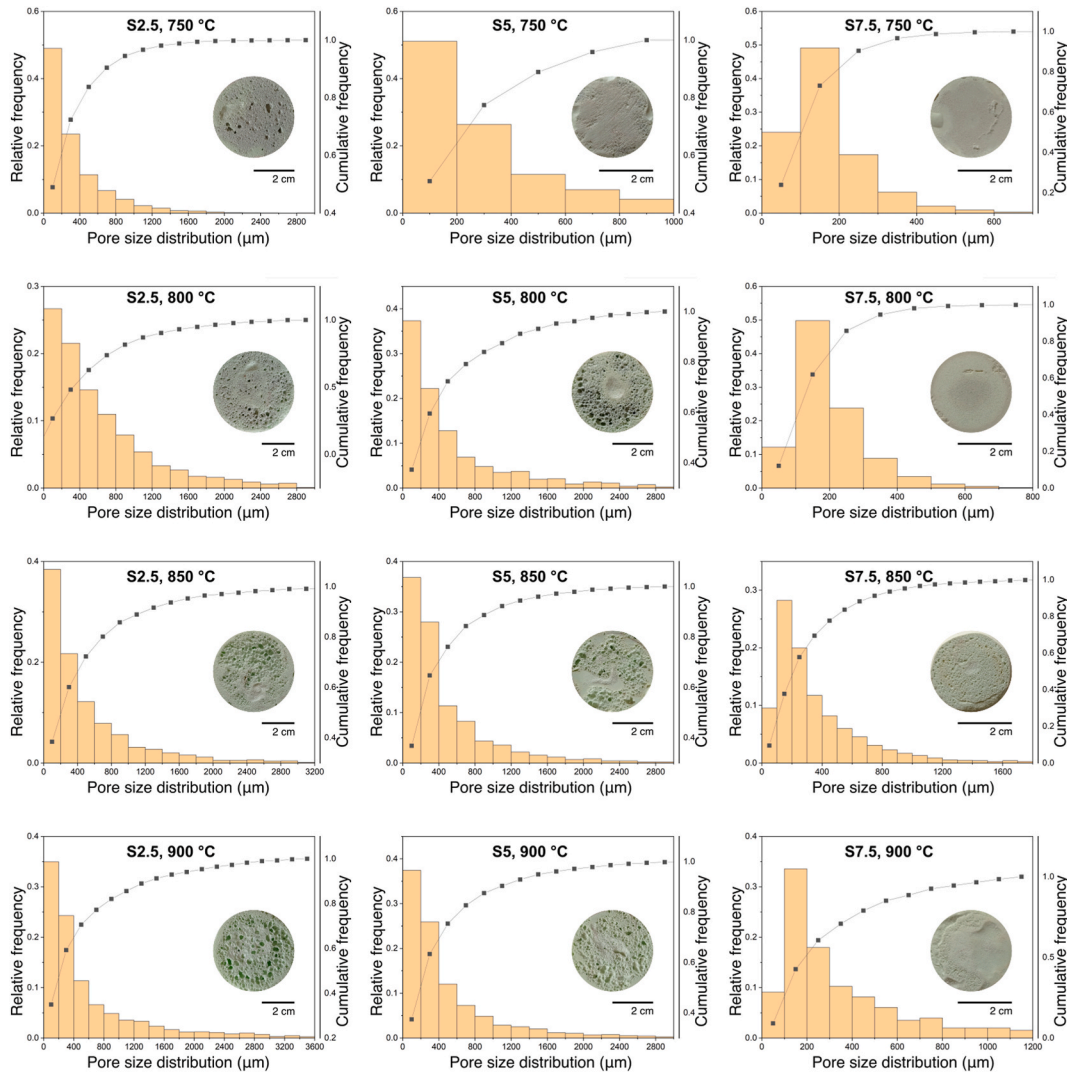
Fig. 5. Digital photographs and pore size distribution of foam glasses sintered at different temperatures.

3.3. Comparison to other construction and insulating materials

Foam glasses produced in this research can find application in the building industry as an environmentally friendly insulating material. The density of different building materials and some research on foam glasses as a function of thermal conductivity is shown in Fig. 6.

It can be seen from Fig. 6 that application of insulating materials can reduce the thermal conductivity of buildings' envelope, meaning that energy consumption can be reduced for heating or cooling of the buildings. The very low thermal conductivity of insulating materials can improve the energy efficiency of buildings envelopes built with traditional construction materials. It can be observed that produced foam glasses have very low thermal conductivity, similar to polystyrene foams and rock wool. Although foam glass synthesized in this research has greater density and thermal conductivity than polystyrene foams and rock wool it has some benefits for a potential application. Foam glass has a higher resistance to fire than polystyrene foams [41] and raw materials are "free of charge" because it is produced entirely from secondary raw materials. It can be produced as panels, easy and safe to handle and install.

4. Conclusion

The foam glass was successfully prepared using only secondary raw materials, green bottle glass as the glass matrix, and SBFL as a foaming agent. SBFL showed that it can be a novel and environmentally friendly substitution for reagent grade $CaCO_3$ for foam glass production. Different amounts of SBFL were added to examine the influence of foaming agent addition on the properties of foam
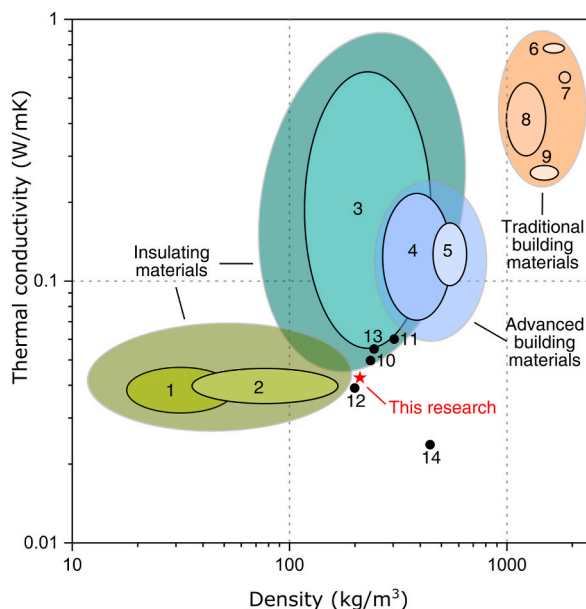
Fig. 6. Density vs Thermal conductivity for: 1- polystyrene foams, 2- rock wool [41], 3- cork board, 4- foamed concrete, 5- aerated concrete, 6- fired bricks, 7- lime sand bricks, 8- lightweight concrete, 9- concrete hollow bricks [42], 10- [20], 11- [24], 12- [26], 13- [21], 14- [43] ★- S2.5 sintered at 800 °C.

glasses at different sintering temperatures. At 750 °C pores didn't fully grow. At higher sintering temperatures $CaCO_3$ from SBFL fully decomposes. The greatest porosity (91.9%) and the lowest density (0.211 g/cm^3) has S2.5 sintered at 800 °C. This sample also shows the lowest thermal conductivity, 0.043 W/(m·K), and compressive strength of 0.63 MPa. These properties of obtained foam glass are comparable to commercial products. Sintering at temperatures of 850 °C and 900 °C doesn't improve the porosity and thermal conductivity of foam glasses. Open-loop recycling of secondary raw materials used in this research can contribute to the sustainable utilization of waste materials for the production of thermal insulators. At the same time reduction of waste disposal, sustainable development, and economic benefits can be achieved.

Author contribution statement

Veljko Savić: Conceived and designed the experiments; Performed the experiments; Analyzed and interpreted the data; Contributed reagents, materials, analysis tools or data; Wrote the paper.

Vladimir Topalović: Analyzed and interpreted the data; Contributed reagents, materials, analysis tools or data.

Jelena Nikolić, Sanja Jevtić, Nebojša Manić: Performed the experiments.

Mirko Komatina: Contributed reagents, materials, analysis tools or data.

Srđan Matijašević: Analyzed and interpreted the data.

Snežana Grujić: Conceived and designed the experiments; Analyzed and interpreted the data; Wrote the paper.

Data availability statement

Data will be made available on request.

Declaration of competing interest

The authors declare that they have no known competing financial interests or personal relationships that could have appeared to influence the work reported in this paper.

Acknowledgments

References

[1] R.K. Dhir, J. de Brito, G.S. Ghataora, C.Q. Lye, Production and Properties of Glass Cullet, 2018, https://doi.org/10.1016/b978-0-08-100984-0.00003-5.
[2] FEVE, EU Glass Packaging Closed Loop Recycling Steady at 74%, Press Release, 2018. https://feve.org/wp-content/uploads/2018/04/Rec-Stats-2015-Press-Release-FINAL.pdf. (Accessed 25 January 2022).
[3] EPA, Glass: Material-specific Data, EPA., 2020. https://www.epa.gov/facts-and-figures-about-materials-waste-and-recycling/glass-material-specific-data. (Accessed 13 September 2022).
[4] SEPA, IZVEŠTAJ O UPRAVLjANjU AMBALAŽOM I AMBALAŽNIM OTPADOM U 2021, GODINI, 2022, p. 23. http://www.sepa.gov.rs/download/Ambalaza_2021.pdf. (Accessed 17 January 2023).
[5] C. Holcroft, M. Pudner, Glass Market Development Assessments for the English Regions and the Nations, Waste & Resources Action Programme, Banbury, Oxon, UK, 2007.
[6] G. Meylan, H. Ami, A. Spoerri, Transitions of municipal solid waste management. Part II: hybrid life cycle assessment of Swiss glass-packaging disposal, Resour. Conserv. Recycl. 86 (2014) 16–27, https://doi.org/10.1016/j.resconrec.2014.01.005.
[7] M. Cheng, M. Chen, S. Wu, T. Yang, J. Zhang, Y. Zhao, Effect of waste glass aggregate on performance of asphalt micro-surfacing, Construct. Build. Mater. 307 (2021), 125133, https://doi.org/10.1016/j.conbuildmat.2021.125133.
[8] H. Hamada, A. Alattar, B. Tayeh, F. Yahaya, B. Thomas, Effect of recycled waste glass on the properties of high-performance concrete: a critical review, Case Stud. Constr. Mater. 17 (2022), e01149, https://doi.org/10.1016/j.cscm.2022.e01149.
[9] K. Mohammedsaleh, R. Kurtulus, Z.A. Alrowaili, T. Kavas, E. Kavaz, M.S. Al-buriahi, Optik Optical properties , elastic moduli , and radiation shielding performance of some waste glass systems treated by bismuth oxide, Optik 266 (2022), 169567, https://doi.org/10.1016/j.ijleo.2022.169567.
[10] J. Feng, D. Wu, M. Long, K. Lei, Y. Sun, X. Zhao, Diopside glass-ceramics were fabricated by sintering the powder mixtures of waste glass and kaolin, Ceram. Int. 48 (2022) 27088–27096, https://doi.org/10.1016/j.ceramint.2022.06.020.
[11] F. Ascione, N. Bianco, G. Maria Mauro, D.F. Napolitano, Building envelope design: multi-objective optimization to minimize energy consumption, global cost and thermal discomfort. Application to different Italian climatic zones, Energy 174 (2019) 359–374, https://doi.org/10.1016/j.energy.2019.02.182.
[12] X. Meng, Y. Huang, Y. Cao, Y. Gao, C. Hou, L. Zhang, Q. Shen, Optimization of the wall thermal insulation characteristics based on the intermittent heating operation, Case Stud. Constr. Mater. 9 (2018), e00188, https://doi.org/10.1016/j.cscm.2018.e00188.
[13] D.M.S. Al-Homoud, Performance characteristics and practical applications of common building thermal insulation materials, Build. Environ. 40 (2005) 353–366, https://doi.org/10.1016/j.buildenv.2004.05.013.
[14] M. Scheffler, P. Colombo (Eds.), Cellular Ceramics: Structure, Manufacturing, Properties and Applications, WILEY-VCH Verlag GmbH & Co. KGaA, Weinheim, 2005.
[15] R.R. Petersen, J. König, Y. Yue, The viscosity window of the silicate glass foam production, J. Non-Cryst. Solids 456 (2017) 49–54, https://doi.org/10.1016/j.jnoncrysol.2016.10.041.
[16] J. König, R.R. Petersen, N. Iversen, Y. Yue, Suppressing the effect of cullet composition on the formation and properties of foamed glass, Ceram. Int. 44 (2018) 11143–11150, https://doi.org/10.1016/j.ceramint.2018.03.130.
[17] J. König, R.R. Petersen, Y. Yue, D. Suvorov, Gas-releasing reactions in foam-glass formation using carbon and MnxOy as the foaming agents, Ceram. Int. 43 (2017) 4638–4646, https://doi.org/10.1016/j.ceramint.2016.12.133.
[18] S. Abbasi, S.M. Mirkazemi, A. Ziaee, M. Saeedi Heydari, The effects of Fe2O3 and Co3O4 on microstructure and properties of foam glass from soda lime waste glasses, Glas, Phys. Chem. 40 (2014) 173–179, https://doi.org/10.1134/S1087659614020023.
[19] R.R. Petersen, J. König, M.M. Smedskjaer, Y. Yue, Effect of Na2CO3 as foaming agent on dynamics and structure of foam glass melts, J. Non-Cryst. Solids 400 (2014) 1–5, https://doi.org/10.1016/j.jnoncrysol.2014.04.029.
[20] J. König, R.R. Petersen, Y. Yue, Influence of the glass-calcium carbonate mixture's characteristics on the foaming process and the properties of the foam glass, J. Eur. Ceram. Soc. 34 (2014) 1591–1598, https://doi.org/10.1016/j.jeurceramsoc.2013.12.020.
[21] M.T. Souza, B.G.O. Maia, L.B. Teixeira, K.G. de Oliveira, A.H.B. Teixeira, A.P. Novaes de Oliveira, Glass foams produced from glass bottles and eggshell wastes, Process Saf. Environ. Protect. 111 (2017) 60–64, https://doi.org/10.1016/j.psep.2017.06.011.
[22] Y. Gong, R. Dongol, C. Yatongchai, A.W. Wren, S.K. Sundaram, N.P. Mellott, Recycling of waste amber glass and porcine bone into fast sintered and high strength glass foams, J. Clean. Prod. 112 (2016) 4534–4539, https://doi.org/10.1016/j.jclepro.2015.09.052.
[23] M. Assefi, S. Maroufi, I. Mansuri, V. Sahajwalla, High strength glass foams recycled from LCD waste screens for insulation application, J. Clean. Prod. 280 (2021), https://doi.org/10.1016/j.jclepro.2020.124311.
[24] S. Arcaro, B.G. De Oliveira Maia, M.T. Souza, F.R. Cesconeto, L. Granados, A.P.N. De Oliveira, Thermal insulating foams produced from glass waste and banana leaves, Mater. Res. 19 (2016) 1064–1069, https://doi.org/10.1590/1980-5373-MR-2015-0539.
[25] N.P. Stochero, J.O.R. de Souza Chami, M.T. Souza, E.G. de Moraes, A.P.N. de Oliveira, Green glass foams from wastes designed for thermal insulation, Waste and Biomass Valorization 12 (2021) 1609–1620, https://doi.org/10.1007/s12649-020-01120-3.
[26] M. Tramontin Souza, L. Onghero, A. Batista Passos, L. Simão, R. Honorato Piva, W. Longuini Repette, A.P. Novaes de Oliveira, Sustainable glass foams produced with stone waste as a pore-forming agent: assessing the role of heating rate in foamability and glass foams recyclability, J. Clean. Prod. 338 (2022), https://doi.org/10.1016/j.jclepro.2022.130596.
[27] M.A. Rajaeifar, S. Sadeghzadeh Hemayati, M. Tabatabaei, M. Aghbashlo, S.B. Mahmoudi, A review on beet sugar industry with a focus on implementation of waste-to-energy strategy for power supply, Renew. Sustain. Energy Rev. 103 (2019) 423–442, https://doi.org/10.1016/j.rser.2018.12.056.
[28] M.N. Garcia Gonzalez, L. Björnsson, Life cycle assessment of the production of beet sugar and its by-products, J. Clean. Prod. 346 (2022), https://doi.org/10.1016/j.jclepro.2022.131211.
[29] M. Gharieb, A.M. Rashad, An initial study of using sugar-beet waste as a cementitious material, Construct. Build. Mater. 250 (2020), 118843, https://doi.org/10.1016/j.conbuildmat.2020.118843.
[30] U. Soydal, M.E. Marti, S. Kocaman, G. Ahmetli, Evaluation of sugar mill lime waste in biobased epoxy composites, Polym. Compos. 39 (2018) 924–935, https://doi.org/10.1002/pc.24019.
[31] E. Šárka, Z. Bubník, P. Kadlec, A. Veselá-Trilčová, The particle size of carbonation mud, and possibilities for influencing it, J. Food Eng. 87 (2008) 45–50, https://doi.org/10.1016/j.jfoodeng.2007.05.023.
[32] A. Astm, C128-07a standard test method for density, in: Relative Density (Specific Gravity), and Absorption of Fine Aggregate vol. 2007, ASTM Int. West, Conshohocken, PA, 2007.
[33] American Society for Testing and Materials, Standard test method for measurement of thermal effusivity of fabrics using a modified transient plane source (MTPS) instrument, ASTM D7984, ASTM Int. Stand. i (2021) 1–5.
[34] C.A. Schneider, W.S. Rasband, K.W. Eliceiri, NIH Image to ImageJ: 25 years of image analysis, Nat. Methods 9 (2012) 671–675, https://doi.org/10.1038/nmeth.2089.
[35] M. Asadi, Beet-Sugar Handbook, John Wiley & Sons, Inc., Hoboken, New Jersey, 2007, https://doi.org/10.1002/9780471790990.
[36] M.J. Pascual, A. Duran, M.O. Prado, A new method for determining fixed viscosity points of glasses, Phys. Chem. Glasses 46 (2005) 512–520.
[37] S.V. Smiljanić, S.R. Grujić, M.B. Tošić, V.D. Živanović, S.D. Matijašević, J.D. Nikolić, V.S. Topalović, Uticaj la2O3 na strukturu i svojstva stroncijum-boratnih stakala, Chem. Ind. Chem. Eng. Q. 22 (2016) 111–115, https://doi.org/10.2298/CICEQ150213031S.
[38] K.S.P. Karunadasa, C.H. Manoratne, H.M.T.G.A. Pitawala, R.M.G. Rajapakse, Thermal decomposition of calcium carbonate (calcite polymorph) as examined by in-situ high-temperature X-ray powder diffraction, J. Phys. Chem. Solid. 134 (2019) 21–28, https://doi.org/10.1016/j.jpcs.2019.05.023.
[39] E.D. Zanotto, Surface crystallization kinetics in soda-lime-silica glasses, J. Non-Cryst. Solids 129 (1991) 183–190, https://doi.org/10.1016/0022-3093(91)90094-M.

[40] M.B. Østergaard, R.R. Petersen, J. König, H. Johra, Y. Yue, Influence of foaming agents on solid thermal conductivity of foam glasses prepared from CRT panel glass, J. Non-Cryst. Solids 465 (2017) 59–64, https://doi.org/10.1016/j.jnoncrysol.2017.03.035.

[41] D. Kumar, M. Alam, P.X.W. Zou, J.G. Sanjayan, R.A. Memon, Comparative analysis of building insulation material properties and performance, Renew. Sustain. Energy Rev. 131 (2020), 110038, https://doi.org/10.1016/j.rser.2020.110038.

[42] H. Zhang, Building Materials in Civil Engineering, 2011, https://doi.org/10.1533/9781845699567.

[43] S.S. Owoeye, G.O. Matthew, F.O. Ovienmhanda, S.O. Tunmilayo, Preparation and characterization of foam glass from waste container glasses and water glass for application in thermal insulations, Ceram. Int. 46 (2020) 11770–11775, https://doi.org/10.1016/j.ceramint.2020.01.211.